

# Deformation During the Electrosurgical Vessel Sealing Process

H. L. Wyatt\*, R. Pullin\*, T. H. J. Yang<sup>†</sup> and S. L. Evans\*

\*Cardiff School of Engineering, Cardiff University, Queen's Buildings, The Parade, Cardiff CF24 3AA, UK

<sup>†</sup>Gyrus Medical Ltd, Fortran Road, St. Mellons, Cardiff CF3 0LT, UK

**ABSTRACT:** Electrosurgical vessel sealing is used throughout many surgical procedures with the benefits of the device widely reported. However, there is still significant variation in the quality of the resulting seal with limited understanding as to why. This study developed a methodology to use digital image correlation to capture the sealing process and to investigate the changes occurring throughout. Porcine carotid arteries were used throughout the study, with seals created using the Gyrus G400 generator and the PKS Open Seal device (Gyrus Medical Ltd, Cardiff, United Kingdom).

The displacement across the surface of the blood vessel and the device jaws was measured, and the true maximum principal strain was computed. There was significant contraction of the tissue along the length of the blood vessel, with this occurring in pulses due to the waveform used to deliver the current. Additionally, there was a significant change in displacement between the device jaws (0.08 mm), a novel finding of the study. This change in displacement is indicative of a change in application force throughout sealing, which can have significant implications in the quality of the seal, and therefore the findings of this study can influence future device design.

**KEY WORDS:** *blood vessels, DIC, electrosurgery, strain*

## Introduction

Electrosurgical vessel sealing devices are used to achieve haemostasis during a variety of surgical procedures including hysterectomies and pulmonary resections [1]. These devices are used as an alternative to more traditional methods such as sutures and staples, with electrosurgical devices providing many benefits to both the practitioner and the patient including reduced patient blood loss, reduced operative time and reduced patient recovery time [2, 3]. Such devices work by passing a high frequency alternating current through the tissue, in turn causing the tissue to heat up and the collagen within the vessel walls to denature. This denatured collagen forms a gel-like substance acting as a glue between the vessel walls, and through the application of force, the seal is formed. Although the benefits of such devices are widely reported, there is still significant variation in the quality of the seal produced [1, 4].

A number of factors have been shown to affect the quality of the seal, with the quality of the seal typically being defined by the seal burst pressure. This is the highest pressure a seal can withstand before there is a sudden and rapid drop in pressure. The vessel size and vessel morphology have been demonstrated to have a significant effect on the quality of the seal. In general, vessels with a larger outer diameter, typically larger than 5 mm, tend to result in a poor seal quality, and vessels with a smaller outer diameter result in seals of a higher quality [5]. Additionally, vessels with a higher elastin content lead to seals of poor quality when compared to seals performed on vessels with a lower elastin content [6], although it should be noted that larger vessels tend to be more elastic by nature, and

therefore it is difficult to be certain of the effect of size and morphology independently of one another. There are many more parameters that are known to affect the quality of the seal, for example, the compressive pressure applied to the seal by the device and the current waveform [7–10]. Although research has demonstrated that factors such as these affect the quality of the seal, there is little understanding as to why these various parameters affect the seal quality, or the changes that occur during the sealing process.

To further study the changes that occur in the tissue during the sealing process and how the various factors affect this process, digital image correlation (DIC) was used to investigate the behaviour of the outer surface of the blood vessel and the behaviour of the device jaws. DIC is a non-contact optical method that can be used to measure displacement and hence to calculate strain. Through the application of a high contrast speckle pattern to the surface of the specimen, the system tracks the various points across the surface, measuring the displacement. By acquiring images before the specimen is loaded and during the loading process, the software can compare the images and produce displacement maps and thus allow strain to be computed [11–13]. This method has many applications in biological tissues including investigating the rupture of aortic aneurysms [14, 15], monitoring the loosening in cemented total hip replacements [11] and characterising the mechanical properties of human skin [16].

The main aim of the study was therefore to develop a suitable methodology for using DIC to capture the vessel sealing process and subsequently to use this method to capture deformation during vessel sealing. The data from the DIC were then used to investigate the changes occurring

to both the blood vessel and the device during the sealing process. The results from this study found significant contraction of the tissue along the length of the blood vessel, with this contraction occurring in pulses. In addition to tissue contraction, the gap between the device jaws varied throughout sealing, with this variation occurring in pulses. This is a novel finding of the study and has implications for future device design.

## Materials and Methods

### Specimen preparation

Porcine carotid arteries, from pigs aged 4–6 months old, were obtained from a local abattoir for testing. Blood vessels were skeletonised using surgical scissors to remove connective tissue and then sectioned. Blood vessels were split into 40-mm sections with the seals being located 25 mm and 65 mm from the bifurcation. It is important to note that the properties of the vessel vary along the length; at 25 mm from the bifurcation, the vessel is typically highly elastic with a large diameter; and at 65 mm from the bifurcation, there is significantly lower elastin content and the vessel has a smaller outer diameter.

Prior to the application of the speckle pattern, it was necessary to pressurise the blood vessel to ensure that the tissue was in tension. The apparatus used to do this consisted of a syringe pump used to deliver saline and a Druck digital pressure indicator to measure the blood vessel pressure. A syringe was fixed into the syringe pump and connected to a three way adaptor. The remaining two outlets of the adaptor were connected to the pressure indicator and a blunt needle used for specimen attachment (Figure 1). The specimen was attached to the blunt needle using a haemostat with the jaws coated in rubber to ensure

a secure connection. Physiological saline (10% w/v) was infused throughout the circuit to ensure all air was removed.

Following the skeletonisation of the blood vessel, the specimens were connected to the saline infusion apparatus using a haemostat. The free end of the specimen was also clamped using a second haemostat to create a small amount of axial tension and to allow the vessel to be pressurised. The blood vessel was pressurised to approximately 60 mmHg, with saline being infused at a rate of  $50 \text{ mL h}^{-1}$ . Once the vessel was pressurised, the speckle pattern was applied. The speckle pattern was applied by first applying a layer of white Snazaroo face paint and subsequently using a make-up brush to sprinkle black make-up powder over the surface of the specimen. In addition to applying the speckle pattern to the blood vessel, the pattern was applied in the same manner over the surface of the upper device jaw. Once the speckle pattern was applied, a trial run was conducted to ensure that the pattern was of sufficient standard to achieve good data collection. This consisted of capturing two images using the DIC system, and processing the data through the software, and checking for gaps within the resulting images.

### DIC equipment set-up and system calibration

The DIC system used was the Q-400 (Dantec Dynamics, Skovlund, Denmark), consisting of the necessary software, Istra4D, a HiLis light source and a data logging system to connect the cameras to the laptop. The HiLis light source is a high intensity LED illumination system, which provides cool and homogeneous illumination. Two digital cameras were used with the system, along with the appropriate lenses (specifications in Table 1). The two cameras were mounted onto a tripod with the HiLis light source positioned between them. The cameras were positioned directly above the specimen to ensure no part of the blood

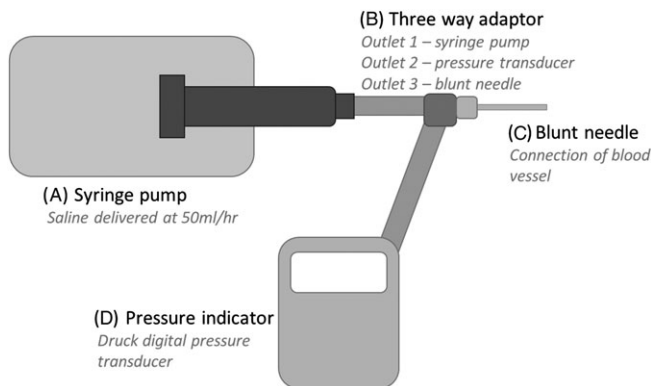


**Figure 1:** Schematic representation of the perfusion circuit used for pressurising the blood vessels for speckle pattern application consisting of a Cole–Parmer syringe pump set at an infusion rate of  $50 \text{ mL h}^{-1}$ , a Druck digital pressure indicator and a blunt needle for attachment of the blood vessel

**Table 1:** Manufacturers specification for the cameras and the lenses used with the digital image correlation system

Camera		Lenses			
Number of cameras	Manufacturer	Name	Magnification range [!:]	Working distance (mm)	Object to image distance (mm)
2	Limess	XNP 2.0/28	>5.9	>174	>232
		Compact			

vessel was obscured during the sealing process (Figure 2). The two cameras were connected to a data logging system, which in turn was connected to the laptop. Following this, the aperture and focus of both cameras were adjusted, with the cameras focused on a rubber tube with a speckle pattern applied to simulate the blood vessel throughout the set-up procedure. To ensure that the vessel sealing device did not move during the analysis, the device was mounted using a clamp and stand.

Following the set-up of the DIC system, it was necessary to conduct a calibration. This determined the position and orientation of each of the cameras with respect to the surface of the specimen and related the pixel size of the object image to the metric scale. In order to calibrate the system, a series of eight calibration images were taken of a calibration target. The calibration target used for this study was a 9 × 9 grid, 40 mm × 40 mm (Dantec Dynamics). The target was rotated and tilted for each image to allow the software to determine the required parameters. A calibration residuum of <0.1 was considered acceptable. The specifications of the calibrated DIC system are presented in Table 2, resulting in a minimum measurable displacement of 0.0052 mm and a strain of 0.0065e.

### Creating and capturing deformation during an electrosurgical seal

To create the electrosurgical seal, the PKS Open Seal device and the Gyrus G400 generator were used. The generator modulates and controls the waveform used to deliver the current to the tissue, with a pulsed waveform supplied to the device. The pulsed waveform has 'off' periods where no current is supplied to the tissue. The device acts as the interface through which the current is delivered to the tissue. Throughout this study, the standard generator setting of VP2 60 was used; this is a vapour pulse coagulation

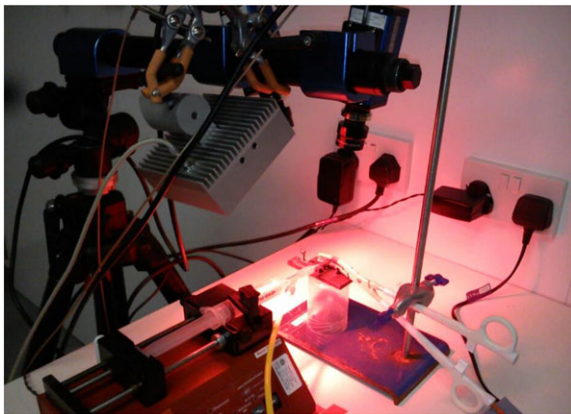


**Figure 2:** Image of the DIC system with two cameras positioned above the specimen. The HiLiS light source was positioned between the two cameras, and the vessel sealing device was clamped to maintain consistent position

**Table 2:** Parameters for the digital image correlation data capture and processing

Technique used	Digital image correlation
Calibration residuum	<0.1
Displacement noise	0.0052 mm
Subset	17 pixels
Total number of images	30 (5 Hz)
Displacement	
Spatial resolution	17 pixels (0.425 mm)
Strain	
Smoothing method	None applied

waveform for intermediate impedance tissue, with 60 referring to the power of the waveform.

To perform an electrosurgical seal, the blood vessel was placed between the jaws of the device. The device was then clamped shut using the ratchets located on the handles, thus providing a consistent and repeatable user technique. The blood vessel was placed within a marked region on the jaws of the device to ensure minimal variation in the application force. It should be noted, however, that application force was not measured as the sealing technique used was designed to be as similar as possible to surgical technique. Subsequently, the device was activated through a footswitch connected to the generator. Upon activation, the generator began to beep, allowing the user to know the device was activated and current was being applied to the tissue. Once the vessel was sealed, there was a tone change from the generator, signalling for the user to remove their foot from the footswitch thus deactivating the device. The duration and applied current varied for each seal due to the feedback controlled system within the generator, with the generator monitoring the tissue impedance to determine when the seal was complete.

The sealing process was captured using the DIC system, with the process being captured at a frame rate of 5 Hz. In total, a 6s period was captured, with the system beginning to capture images approximately 2s prior to the activation of the generator. Typically, coagulation waveforms have a duty cycle of around 6% [17], meaning that the current is only on for 6% of the time, suggesting that a frame rate of 5 Hz would be sufficient to capture the sealing process. The sealing process typically lasts 2–3s, with around 1–2s being captured after the sealing process was complete. Images captured after the sealing process was complete had no heat applied, with the generator deactivated or in the 'off' mode. The deformation of the vessel typically reached a steady state within this period, before image collection stops. Images were captured using an automated triggering feature within the Istra4D software.

## Data processing

Data were processed within the DIC software, Istra4D, with the parameters from capture and processing displayed in Table 2. A mask was drawn covering both the surface of the jaws and the surface of the blood vessel, with these two areas being defined as the areas of interest. Two start points were defined for each sample, one located on the jaws and one on the vessel. The start point was a point which could be found within all captured images of the specimen to allow the software to conduct the necessary calculations and processing. Within each data set, axes were defined for the samples, with the  $y$ -axis pointing along the length of the blood vessel, the  $x$ -axis defined to be parallel to the bottom edge of the device jaw and the  $z$ -axis defining the out of plane direction. For each sample, the  $z$  displacement for the device jaws, the  $y$  displacement for the tissue and the true maximum principal strain for the tissue were considered.

When processing the  $y$  displacement of the tissue, a line was drawn across the width of the vessel, 5.5–6 mm from the edge of the device jaws (Figure 3). The mean  $y$  displacement of this line was exported from Istra4D for processing in Excel. This allowed for the comparison of the mean  $y$  displacement amongst the different samples and allowed for consistency in the processing of the results. Additionally for the tissue, the true maximum principal strain for all samples was computed. When processing the

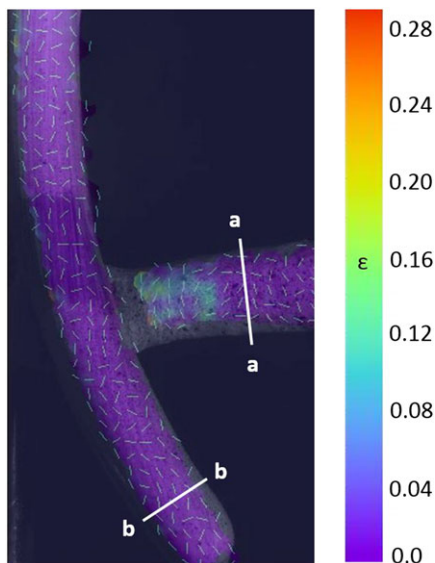


**Figure 3:** Image showing true maximum principal strain during the initial stages of sealing, with the small lines within the strain map showing the local orientation of the strain. Axes were defined with the  $y$ -axis pointing along the length of the blood vessel, the  $x$ -axis defined to be parallel to the bottom edge of the device jaw and the  $z$ -axis defining the out of plane direction. Line aa shows the line used when processing the tissue data, and line bb shows the line used when processing the jaw data

displacement of the device jaws, it was the  $z$  displacement that was of interest, and a similar approach was used. A line was drawn across the width of the jaws, 1.5–2 mm from the distal end of the jaws (Figure 3), with the mean  $z$  displacement exported from Istra4D to Excel.

## Results

The use of DIC proved to be successful. The method allowed for changes occurring in both the device and the tissue to be assessed. When considering the results from the investigation, the displacement will first be considered for both the device jaws and the tissue, followed by the true maximum principal strain at the tissue surface.

Figure 4 shows the displacement of the device jaws for six seals captured using DIC. Significant displacement occurred for the device jaws in the  $z$  direction. For all samples, this change in displacement occurred in pulses, with all but one sample resulting in an overall negative  $z$  displacement. A negative  $z$  displacement is indicative of compression or shrinkage of the tissue between the device jaws. For the specimen that ended with a positive displacement, it is thought that sealing continued beyond the DIC data capture for that specimen. The pulsating of the device jaws throughout the sealing process is a novel finding of the study. The maximum change in the displacement of the device jaws was indicative of an  $\approx 15\%$  change (0.8 mm) in the gap between the two jaws of the device. For all samples, the initial gap between the jaws of the device was consistent, with the gap being controlled by a nylon stopper located between the device jaws. The variation in the jaw gap is an important finding due to the influence of this gap on the application force throughout sealing. The dotted lines shown in Figure 4 show seals performed at 25 mm from

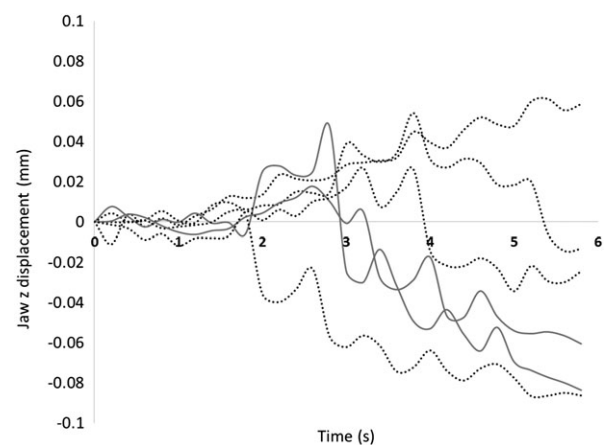


**Figure 4:** The  $z$  displacement of the jaws during the sealing process. A positive change in displacement indicates an increase in the shim gap. Each line refers to a different seal performed, with dotted lines referring to specimens sealed at 25 mm from the bifurcation and solid lines showing seals performed at 65 mm from the bifurcation

the bifurcation, with solid lines showing seals performed at 65 mm from the bifurcation. As seen in Figure 4, there appears to be no trend in terms of jaw displacement and the morphology of the vessel, although the sample size is relatively small.

Figure 5 shows the  $y$  displacement of the sealed blood vessel for five seals captured using DIC. Figure 5 shows significant change in the displacement of the tissue along its axis ( $y$  direction), with positive  $y$  displacement indicating tissue contraction with the tissue being pulled towards the jaws of the device. Both the  $y$  displacement and the  $y$  strain were considered when investigating vessel behaviour, with both data sets showing similar trends; however, for the purpose of this study, only the  $y$  displacement data were presented due to the increase in noise within the strain data due to the DIC method.

Similarly to Figure 4, the different line types within Figure 5 represent different seal locations (dotted lines show seals at 25 mm, and solid lines show seals at 65 mm from the bifurcation). Figure 5 shows no trend in terms of the tissue displacement and the morphology of the vessel. Similarly to the displacement of the jaws, the displacement of the tissue occurs in pulses. Figure 6 shows that the pulses in both the displacement of the jaws and tissue occur simultaneously.

Figure 7 shows an example of the true maximum principal strain of the blood vessel at various stages throughout the sealing process. Figure 7A shows the initial image prior to the start of the sealing process. This image shows the true maximum principal strain orientated in random directions due to the lack of loading, essentially showing the noise in the data. Figure 7B shows the image at 2.4 s, when the sealing had just began. As can be seen with this image, the true principal strain of the blood vessel in the area adjacent to the jaw was orientated in the  $x$  direction, showing an

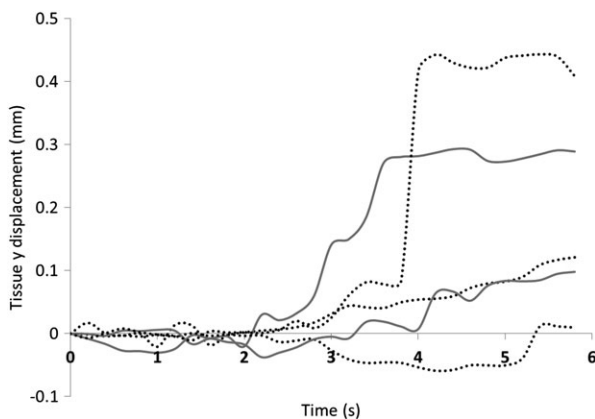


**Figure 5:** The  $y$  displacement of the tissue during the sealing process. A positive change in displacement indicates the tissue moving closer to the device. The dotted lines referring to specimens sealed at 25 mm from the bifurcation and solid lines showing seals performed at 65 mm from the bifurcation

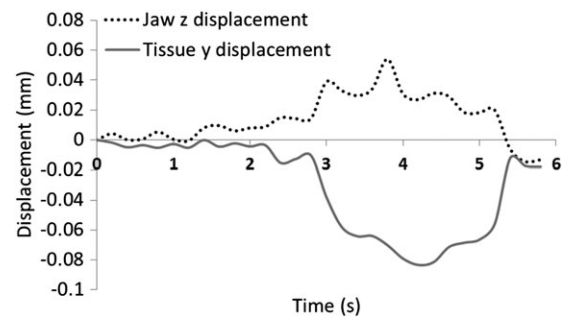


**Figure 6:** An example of the  $y$  displacement of the tissue and the  $z$  displacement of the jaws during the sealing process. A positive change in tissue displacement indicates the tissue moving closer to the device, and a positive change in jaw displacement indicates an increase in shim gap

increase in vessel width. As the sealing progressed, the true principal strain along the vessel gradually became orientated in the  $y$  direction (Figure 7C) and at the final stages of sealing, the true principal strain along the entire length was principally in the  $y$  direction (Figure 7D). This gradual change in orientation of the true principal strain of the vessel was seen in all tested samples.

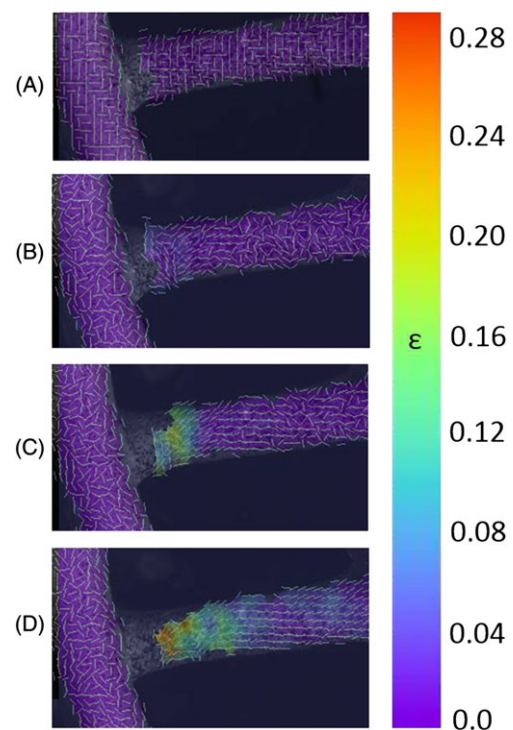


**Figure 7:** Images showing sequential stages of the sealing process, with the blood vessel orientated with the shim on the left-hand side. Image (A) was taken at 0 s, image (B) at 2.4 s, image (C) at 3.6 s and image (D) at 4 s. Images show the strain map for the true maximum principal strain, with the small lines within the strain map showing the local orientation of the strain. All images using the same scale bar indicated on the right-hand side

## Discussion

The study developed a methodology for using DIC to capture the electrosurgical vessel sealing process, providing a valuable insight into the changes occurring throughout sealing. Additionally, the results from the study presented a number of novel findings, including the pulsating of the device jaws, which has the potential to influence future device design. This is the first time such a technique has been used to capture the sealing process, and as such, the method used highlighted many issues and complexities that were previously unknown. The main difficulty with developing the methodology was due to the high level of deformation occurring during the sealing process; this is a common problem when working with soft tissues [11]. The high level of deformation made it difficult to analyse the changes in the tissue in the area adjacent to the sealing device; this is the region of the tissue where the greatest amount of contraction, shrinkage and deformation occurs. Due to the large level of deformation occurring within the vessel, there is a lot of distortion of the speckle pattern, with large areas of white space emerging as the vessel deforms. This makes it difficult for the software to create a full displacement or strain map over the surface of the specimen. In addition, this large change in the tissue occurs over a short period in time, typically around 2 s, creating further difficulty when using the system. It is thought that using a high speed DIC system would allow more detail to be captured throughout the sealing process and would reduce the difficulties in analysing the large changes occurring in the area adjacent to the device, although this would not eradicate all problems as the problem would remain one with high levels of deformation.

The preparation and treatment of the blood vessel were also a key part of the development of the method. The blood vessel was skeletonised to remove most connective tissue; this eliminated some of the variation between samples and allowed for more consistent sealing and measurement of surface movement and was an essential part of the specimen preparation. The loading conditions of the vessel can also affect how the vessel behaves, and therefore, it was important to keep these consistent through the different tests. Throughout this study, a small amount of axial tension was applied to the blood vessel; this was to allow for the speckle pattern to be applied and was essential in ensuring that the pattern was of sufficient quality for testing. The speckle pattern was applied to the blood vessel using a combination of white face paint and black powder, with this method proving to be an excellent way of applying the pattern to the tissue.

Through the development of the methodology and the processing of the DIC data, a number of key findings regarding the changes occurring during the electrosurgical sealing process were made. When considering the behaviour

of the tissue throughout the process, there was considerable contraction of the tissue in the axial direction ( $y$ -axis, Figure 5) with this contraction occurring in pulses. The contraction of the tissue was to be expected due to the shrinking of the collagen fibres that occurs as a result of the tissue heating up [18–20]. The results further demonstrated both contraction (positive  $y$  displacement) and relaxation (negative  $y$  displacement) of the tissue in the axial direction, with this change occurring in pulses. This pulsating of the tissue is thought to be caused by the pulsing of the generator waveform and the resulting temperature of the tissue. When the tissue reaches the required temperature ( $\approx 70^\circ\text{C}$ ), created during one of the 'on' periods of the generator waveform, the collagen within the vessel wall denatures, resulting in the contraction of the tissue. During the 'off' period of the generator waveform, the tissue is allowed to cool slightly, and the tissue relaxes. This relaxation is thought to be due to the collagen that was not denatured returning back to its original wavy state.

Additionally, the magnitudes of the  $y$  and  $z$  displacements and the true maximum principal strain were considered for all samples to further explore the effects of vessel properties on the sealing process. A previous study had found that as the distance from the bifurcation of the vessel increased, the amount of elastin and the diameter of the blood vessel reduced, and the quality of the seal improved [21]. Therefore, vessels sealed at 25 mm from the bifurcation could be considered larger, more elastic, with a weaker seal than the vessels sealed at 65 mm. When considering the magnitude of the displacements and strains, no trend could be seen based on the position of the seal, indicating that these parameters were not indicative of seal quality or determined by these vessel properties. It should be noted, however, that a larger sample size would be required to fully investigate these relationships.

The behaviour of the tissue was further analysed by considering the maximum principal strain on the tissue surface. By considering the principal strain, it became apparent that for all samples, there was an initial expansion of the blood vessel in the  $x$  direction, parallel to the device jaws, indicating an increase in the width of the vessel. This initial increase in vessel width was unexpected and suggests further complexities to the vessel sealing process, with one possible explanation of this expansion being due to the increased fluid volume due to the thermal expansion of water within the vessel wall. Following the initial expansion in vessel width, there was a gradual change in the orientation of the true maximum principal strain (Figure 7). As the sealing progressed, the tissue adjacent to the jaws had the maximum principal strain in the  $x$  direction, and further away from the jaws, the strain started to orientate itself in the  $y$  direction. As the sealing entered its final stages, the strain was orientated in the  $y$  direction along the entire length of the vessel. This orientation of the

principal strain in the  $y$  direction justified considering the  $y$  displacement when analysing the tissue behaviour as this was the most significant displacement that occurred, in terms of magnitude during the sealing process.

Furthermore, when considering the strain distribution throughout the sealing process, vessels displayed an uneven strain distribution across the surface of the vessel. The strain varied between specimens, with larger strain magnitudes occurring on either edge of the vessel wall (either the edge close to the distal end of the device jaws or the edge near the pivot point of the device jaws, Figure 7). This was unexpected as the position of the larger strain magnitude varied amongst samples, always favouring one edge of the vessel. This is thought to be caused by a variation in the thickness of the vessel wall, with thinner regions of the vessel wall allowing the current to take the path of least resistance, resulting in greater contraction within that region. As the tissue was heated, and the collagen was denatured, the resistance of the tissue increased, and therefore the thicker regions of the vessel wall became the path of least resistance. This effect shows that the sealing process varies within each seal, and that to achieve consistency from one seal to the next is a very complex challenge.

In addition to considering the deformation of the tissue, by applying a speckle pattern to the device jaws, their movement could be considered. Figure 4 shows significant displacement of the device jaws in the  $z$  direction, out of plane movement, with this displacement also occurring in pulses. This displacement caused a maximum variation in the gap between the device jaws of  $\approx 15\%$ . The gap between the jaws is of great importance as it controls the application force, which is known to significantly influence seal quality. Existing work has shown that too high an application force damages the tissue, and too low an application force is insufficient to create a high-quality seal [7]. A fluctuation in the shim gap indicates a fluctuation in the application force throughout sealing and can therefore reduce the quality of the seal resulting in a lower burst pressure. Furthermore, the fluctuation in the gap varied along the length of the jaws, with the greatest variation seen at the distal end. The results from this analysis highlight the importance of the positioning of the vessel along the length of the jaws when performing a seal, not only due to the application force but also due to the consistency of the shim gap throughout the seal. It is important for users of the device to be aware of this fluctuation and that such differences can have a significant effect on seal quality.

The pulsating of the device jaws and the tissue occurred simultaneously, as shown in Figure 6, with this pulsing being due to the pulsed waveform delivered by the generator. The pulsing of the device jaws was thought to be due to the expansion of water within the vessel wall, with the volume of water increasing by approximately 3%

at 70 °C (predicted using thermal expansion theory). With this expansion of water volume within the blood vessel wall, the pressure between the device jaws increases, forcing the gap between the device jaws to widen. This explains the initial positive  $z$  displacement of the device jaws. During the 'off' periods of current delivery, the water is allowed to cool, decreasing the fluid pressure within the vessel wall, leading to the negative  $z$  displacement seen in Figure 4. Although the pulses of the jaws and the tissue were caused by different phenomena, they coincide with one another due to the relationship with the generator pulses and the tissue temperature.

The work presented within this study provides a useful insight into the changes occurring throughout the electrosurgical sealing process, especially in terms of device performance. The variation in the gap between the device jaws is a novel finding that should be considered in the design of future devices as it can significantly influence the quality of the seal. Additionally, this fluctuation in the gap between the jaws varies along the length of the device, which could significantly influence how the device is used throughout surgery, allowing surgeons to develop their technique accordingly to achieve a more consistent seal quality. This study can be expanded to further explore the sealing process, including increasing the sample size to explore relationships between vessel characteristics, such as diameter and morphology, to try and improve understanding surrounding the variation in seal quality. Similarly, work could vary characteristics of the sealing device, such as the application force and surface features, to understand how these changes influence the quality of the seal and the way in which the seal is formed.

## Conclusion

The study presents a suitable methodology for using DIC to capture the vessel sealing process and demonstrates the benefits of using the technique as it provides a valuable insight into the process. Through the use of DIC, the pulsing of both the device jaws and the tissue was quantified with the fluctuation in the gap between the jaws being a novel finding of this study. The pulsing of the device jaws results in a variation in the compressive pressure and is thought to lead to a fluctuation in temperature throughout the sealing process, which could have a strong influence on seal quality. The pulsing of both the jaws and the tissue was created by the generator waveform and the resulting temperature of the tissue.

By analysing the displacement of both the tissue and the device jaws throughout the sealing process, it has been shown that no two seals were produced in the same way, with a difference being seen in both the magnitude and the pattern of the displacement for both the tissue and the device jaws. The large variation in displacement was to be

expected due to the large variation in the seal quality reported in existing studies. The magnitude of the displacement of the tissue and the jaws did not relate to the vessel properties (morphology and size based on the seal position) and indicate further investigation is needed including creating a larger sample size.

## ACKNOWLEDGEMENTS

The authors would like to thank the Engineering and Physical Sciences Research Council Doctoral Training Grant and Gyrus Medical Ltd for financial support. The authors would also like to thank Dr Mark Eaton and Dr John McCrory for their help and support with the DIC system.

## Data Access Statement

Information about the data that supports this article, including how to access them, can be found in the Cardiff University data catalogue at 10.17035/d.2016.0009096673.

## REFERENCES

1. Massarweh, N. N., Cosgriff, N., and Slakey, D. P. (2006) Electrosurgery: history, principles, and current and future uses. *J. Am. Coll. Surg.* **202**(3), 520–530.
2. van Kesteren, P. (2005) New haemostatic technologies; has conventional ligation become obsolete? *Int. Congress Series* **1279**, 189–191.
3. Pons, Y., et al. (2009) Comparison of LigaSure vessel sealing system, harmonic scalpel, and conventional hemostasis in total thyroidectomy. *Otolaryngol. Head Neck Surg.* **141**(4), 496–501.
4. Presthus, J. B., Brooks, P. G., and Kirchof, N. (2003) Vessel sealing using a pulsed bipolar system and open forceps. *J. Am. Assoc. Gynecol. Laparosc.* **10**(4), 528–33.
5. Carbonell, A. M., Joels, C. S., Kercher, K. W., Matthews, B. D., Sing, R. F., and Heniford, B. T. (2003) A comparison of laparoscopic bipolar vessel sealing devices in the hemostasis of small-, medium-, and large-sized arteries. *J. Laparoendoscopic Adv. Surg. Techniques* **13**(6), 4.
6. Sindram, D., Martin, K., Meadows, J. P., Prabhu, A. S., Heath, J. J., McKillop, I. H., Iannitti, D. A. (2011) Collagen–elastin ratio predicts burst pressure of arterial seals created using a bipolar vessel sealing device in a porcine model. *Surgical Endoscopy*, p. 1–9.
7. Wallwiener, C. W., et al. (2008) Thermal conduction, compression, and electrical current – an evaluation of major parameters of electrosurgical vessel sealing in a porcine in vitro model. *J. Minim. Invasive Gynecol.* **15**(5), 605–610.
8. Richter, S., et al. (2006) Differential response of arteries and veins to bipolar vessel sealing: evaluation of a novel reusable device. *J. Laparoendoscopic & Adv. Surg. Techniques* **16**(2), 149–155.
9. Richter, S., et al. (2006) Efficacy and quality of vessel sealing – comparison of a reusable with a disposable device and effects of clamp surface geometry and structure. *Surg. Endoscopy Other Interventional Techniques* **20**(6), 890–894.
10. Farrugia, M., et al. (2001) Recent advances in electrosurgery – VERSAPOINT® technology. *Rev. Gynaecol. Practice* **1**(1), 12–17.
11. Zhang, D., and Arola, D. D. (2004) Applications of digital image correlation to biological tissues. *J. Biomed. Opt.* **9**(4), 691–699.
12. Zhang, D., Eggleton, C., and Arola, D. (2002) Evaluating the mechanical behavior of arterial tissue using digital image correlation. *Exp. Mech.* **42**(4), 409–416.
13. Sutton, M. A., J. J. Orteu, and Schreier, H. W., (2009) Image correlation for shape, motion and deformation measurements: basic concepts, theory and applications, Springer.
14. Kim, J.-H., et al. (2012) Experimental characterization of rupture in human aortic aneurysms using a full-field measurement technique. *Biomech. Model. Mechanobiol.* **11**(6), 841–853.
15. Romo, A., Badel, P., Duprey, A., Favre, J. P., and Avril, S. (2014) *In vitro* analysis of localised aneurysm rupture. *J. Biomech.* **47**(3), 607–616.
16. Evans, S. L., and Holt, C. A. (2009) Measuring the mechanical properties of human skin *in vivo* using digital image correlation and finite element modelling. *J. Strain Anal. Eng. Design* **44**(5), 337–345.
17. Munro, M. G. (2012) Fundamentals of electrosurgery part I; principals of radiofrequency energy for surgery. In: *The SAGES Manual on the Fundamental Use of Surgical Energy* (Feldman, L., Fuchshuber, P., and Jones, D. B. Eds). Springer, Berlin.
18. Sigel, B., and Acevedo, F. J. (1963) Electrocoaptive union of blood vessels: a preliminary experimental study. *J. Surg. Res.* **3**(2), 90–96.
19. Sigel, B. D., and Marvin, R. (1965) The mechanism of blood vessel closure by high frequency electrocoagulation. *Surgical Gynecol. Obst.* **8**, 9.
20. Winter, H., et al. (2010) Pilot study of bipolar radiofrequency-induced anastomotic thermofusion – exploration of therapy parameters *ex vivo*. *Int. J. Colorectal Dis.* **25**(1), 129–133.
21. Wyatt, H. L., Richards, R., Pullin, R., Yang, T. H. J., Blain, E. J., and Evans, S. L. (2016) Variation in electrosurgical vessel seal quality along the length of a porcine carotid artery. *Proc. Inst. Mech. Eng., H: J. Eng. Med.* **230**, 169–174.